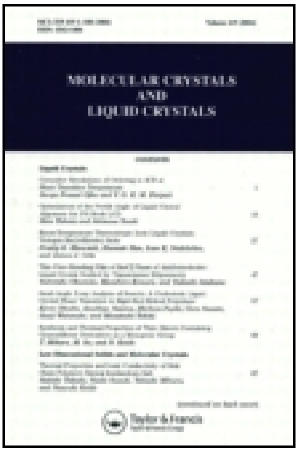

Molecular Crystals and Liquid Crystals Science and Technology. Section A. Molecular Crystals and Liquid Crystals

Publication details, including instructions for authors and subscription information:
http://www.tandfonline.com/loi/gmcl19

New Magnetically Ordered Materials with High T_c

Joel S. Miller [a] & Arthur J. Epstein [b]

[a] Du Pont Science & Engineering Laboratories, Experimental Station E328, Wilmington, DE, 19880-0328, USA

[b] Department of Physics and Department of Chemistry, The Ohio State University, Columbus, OH, 43210-1108, USA

Version of record first published: 05 Dec 2006.

To cite this article: Joel S. Miller & Arthur J. Epstein (1993): New Magnetically Ordered Materials with High T_c, Molecular Crystals and Liquid Crystals Science and Technology. Section A. Molecular Crystals and Liquid Crystals, 233:1, 133-152

To link to this article: http://dx.doi.org/10.1080/10587259308054956

Mol. Cryst. Liq. Cryst. 1993, Vol. 233, pp. 133–152
Reprints available directly from the publisher
Photocopying permitted by license only

Printed in the United States of America

NEW MAGNETICALLY ORDERED MATERIALS WITH HIGH T_C

JOEL S. MILLER
Du Pont Science & Engineering Laboratories, Experimental Station E328,
Wilmington, DE 19880-0328 (USA)

ARTHUR J. EPSTEIN
Department of Physics and Department of Chemistry, The Ohio State University,
Columbus, OH 43210-1108 (USA)

Abstract Magnets comprised of molecules, ions, and polymers is a focus of contemporary materials science research. The anticipated attributes of organic/molecular-based magnetic materials may enable their use in future generations of electronic, magnetic and/or photonic/photronic devices. Some organometallic solids comprising linear chains of alternating metallocenium donors, D, and cyanocarbon acceptors, A, *i. e.*, $\cdots D^{\cdot +}A^{\cdot -}D^{\cdot +}A^{\cdot -}\cdots$, exhibit cooperative magnetic phenomena, *i. e.*, ferro-, antiferro-, ferri-, and metamagnetism. For $[Fe^{III}(C_5Me_5)_2]^{\cdot +}[TCNE]^{\cdot -}$ (Me = methyl; TCNE = tetracyanoethylene) bulk ferromagnetic behavior is observed below the critical (Curie) temperature, T_c, of 4.8 K. Replacement of Fe^{III} with Mn^{III} leads to a ferromagnet with a T_c of 8.8 K in agreement with mean-field models developed for this class of materials. Extension to the reaction of a vanadium(0) complex with TCNE lead to the isolation of a magnet with a $T_c \sim 400$ K which exceeds the thermal decomposition of the material. A new class of metalloporphins exhibiting magnetic order are also reported. This demonstrates that a magnetic material with a T_c substantially above room temperature is achievable in a molecule/organic/polymeric material.

INTRODUCTION

Mankind has benefited from magnets for millennia and continues to do so. In perhaps the earliest example of technology transfer involving condensed matter science the compass was invented.[1] Today magnets are used in magneto-mechanical machines, acoustic devices, telecommunication/information technology, and to motors and generators and consequently are indispensable to our high-tech society. 'Smart' materials and systems of the future will undoubtedly rely upon switches, sensors, and transducers which will be comprised in part by magnetic materials. Thus, magnets materials are a key focus of modern materials research programs.

Magnetic materials of today are composed of d- or f-orbital transition or lanthanide atom/ion-based with an extended network bonding in at least two dimensions and are prepared by high-temperature metallurgy. A molecule-based organic/polymeric materials may permit the selective modulation of the magnetic properties by organic chemistry methods. This may enable the combining of magnetic properties with mechanical, electrical, or optical properties, as well as simplifying the fabrication through low-temperature methods, Table I, to enable the use of organic materials in future generations of electronic, magnetic and/or photonic/photronic devices.

TABLE I Representative Examples of Magnetic Materials

Building Unit	Example [a]	Active Spin Site	Processing Method
Atom-based[b]	Fe, Fe_3O_4, Co_5Sm, CrO_2	Fe, Co, Sm, Cr	Metallurgy
	C	C [c]	Pyrolysis/Metallurgy
Molecule-based	$[FeCp^*_2][TCNE]$	Fe^{III}, TCNE [d]	Growth from solution
	$Mn(hfac)_2(NITR)$	Mn^{II}, ONR [d]	Growth from solution
	$Cu^{II}Mn^{II}(obbz)$	Mn^{II}, Cu^{II}	Growth from solution
	p-$NO_2C_6H_4NIT$	ONR [d]	Growth from solution

[a] Abbreviations are defined later in the text [b] Commercial Products
[c] Proposed [d] p-orbital based

Molecule-based ferromagnetic compounds, although postulated in the 1960's, have characterized only within the past decade.[2-8] Herein we will very briefly describe a few of our recent research results.

STRUCTURE AND MAGNETIC PROPERTIES OF ELECTRON-TRANSFER DONOR/ACCEPTOR SALTS

In 1979 $[Fe^{III}Cp^*_2]^{\cdot+}[TCNQ]^{\cdot-}$ (TCNQ = 7,7,8,8-tetracyano-*p*-quinodimethane, Cp* pentamethylcyclopentadienide, C_5Me_5) was characterized as a metamagnet, *i. e.*, below

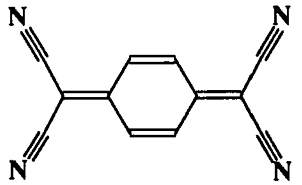

TCNQ

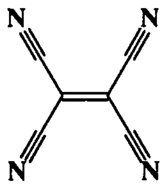

TCNE

1.6 kOe applied field the magnetization is characteristic of an antiferromagnet, whereas above 1.6 kOe a sharp rise and approach to magnetization saturation characteristic of a ferromagnet is observed.[9] The tetracyanoethylene (TCNE) analog was latter characterized has having a bulk ferromagnet ground state.[10] These materials are comprised of alternating cation donors, D, and anion acceptors, A, *i. e.*, $\cdots D^{\cdot+}A^{\cdot-}D^{\cdot+}A^{\cdot-}\cdots$, Figure 1.[6,7]

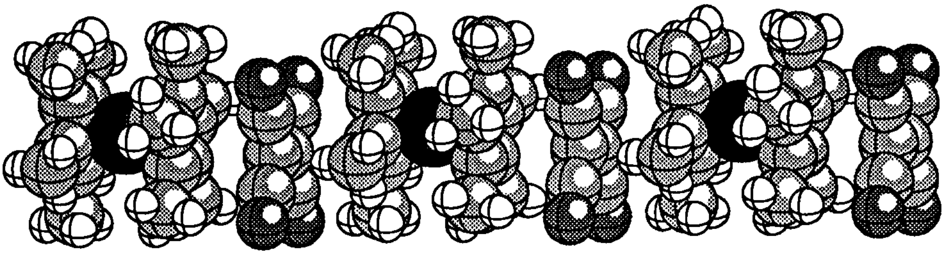

FIGURE 1. $\cdots D^{\cdot+}A^{\cdot-}D^{\cdot+}A^{\cdot-}\cdots$ observed for $[Fe^{III}Cp^*_2]^{\cdot+}[TCNE]^{\cdot-}$ and $[Fe^{III}Cp^*_2]^{\cdot+}[TCNQ]^{\cdot-}$ (not shown).

Though several metamagnets, *e. g.*, $FeCl_2$, had been reported,[11] this was the first example where a 1-, 2- or a 3-D covalently bonded network structure is not present. Thus, we sought to identify the relationship between the structure and magnetic properties by a systematic modification of the acceptor A, the C_5Me_5-ring substituent groups, and the metal-ion to establish the stearic/electronic features necessary to stabilize ferromagnetism and ultimately design a molecular based ferromagnet. On the assumption that a smaller radical anion would have a greater spin density which could permit increased spin-spin interactions, we sought to identify stable radical ions smaller than $[TCNQ]^{\cdot-}$ and selected $[TCNE]^{\cdot-}$.

$[Fe^{III}Cp^*_2]^{\cdot+}[TCNE]^{\cdot-}$ was prepared and also found to possess the $\cdots D^{\cdot+}A^{\cdot-}D^{\cdot+}A^{\cdot-}\cdots$ motif, Figure 1.[6,12] In a zero applied magnetic field a spontaneous magnetization is observed.[6,13] The saturation magnetization for single crystals aligned parallel to the $\cdots D^{\cdot+}A^{\cdot-}D^{\cdot+}A^{\cdot-}\cdots$ stacking axis is 36% greater than on an iron basis and is in agreement with the calculated saturation moment for ferromagnetic alignment of the donor and the acceptor. The Curie (critical) temperature, T_c, was determined to be 4.8 K. A summary of the physical properties can be found in Table II.

Fitting the susceptibility data to different physical models aids in the understanding of the microscopic spin interactions. Above 16 K interactions among the nearest neighbor spins within individual 1-D chains are sufficient to understand the magnetic behavior. The Curie-Weiss Law, $\chi \propto T^{-1}$, is sufficient to model the higher temperature ($T > 130$ K) data with $\theta = 30$ K.[6,12,13] An 1-D Heisenberg model with a ferromagnetic exchange coupling, J, of 19 cm^{-1}, however, models the data down to 16 K.[13] These models, however, are insufficient to explain the magnetic susceptibility below 16 K as long range spin correlations and 3-D spin interactions become increasingly important, until permanent 3-D ferromagnetic order occurs at a T_c of 4.8 K. Variation of the low-field magnetic susceptibility with temperature above T_c, magnetization with temperature below T_c, and the magnetization with magnetic field at T_c enabled a measurement of three critical exponents (Table II) for the magnetic field parallel to the

TABLE II Summary of Properties of the Molecular/Organic Bulk Ferromagnet $[Fe(C_5Me_5)_2]^{\cdot +}[TCNE]^{\cdot -}$

rty	Value
/):	$C_{26}H_{30}FeN_4$ (454.4 daltons)
	1-D $\cdots D^{\cdot +}A^{\cdot -}D^{\cdot +}A^{\cdot -}D^{\cdot +}A^{\cdot -}\cdots$ Chains
	Conventional Organic Solvents (*e.g.*, THF, CH_2Cl_2, MeCN)
Temperature:	4.8 K (+0.21 K/kbar applied pressure up to 14 kbar)
θ Constant $\parallel$ ($\perp$) to 1-D chains:	+30 (+10) K
Magnetization:	Yes - in zero applied field
ceptibility $\parallel$ ($\perp$) to 1-D chains:	0.00667 (0.00180) emu/mol (Observed, 290 K)
ceptibility $\parallel$ ($\perp$) to 1-D chains:	0.00640 (0.00177) emu/mol (Calculated, 290 K)
agnetization $\parallel$ ($\perp$) to 1-D chains:	16,300 (6,000) emuG/mol (Calculated16,700 emuG/mol)
change Interaction $\parallel$ ($\perp$) to 1-D chains):	27.4 K (19 cm^{-1}) [8.1 K (5.6 cm^{-1})]
irves:	Yes (1000 Oe Coercive Field; cf. 1 Oe for iron metal)
stant:	0.09
stant:	~0.5
stant $\parallel$ ($\perp$) to 1-D chains:	1.22 (1.19)
stant:	4.4
c Ordering:	Yes - Neutron Diffraction Studies on polycrystalline-d_{30} samples
ıer Zeeman Splitting:	Yes - in zero applied Field (Large Internal Field: 424,000 G(4.2K)

chain axis. The observed values are in accord with a transition to a 3-D ordered magnetic state.

Recently, the pressure dependence of the T_c for $[FeCp^*_2]^{\cdot+}[TCNE]^{\cdot-}$ has been studied. Preliminary studies of the pressure dependence of T_c reveals that T_c increases with applied pressure by 0.21 K/kbar and reaches 7.8 K at 14 kbar applied pressure.[14] The $[Co^{III}Cp^*_2]^+[TCNE]^{\cdot-}$ complex with a diamagnetic donor has been prepared and exhibits essentially the Curie susceptibility anticipated for $[TCNE]^{\cdot-}$.[12] Additionally, to test of the critical importance of the one-dimensionality, the spinless S = 0 $[CoCp^*_2]^+$ cations were randomly substituted for the cation in $[FeCp^*_2]^{\cdot+}[TCNE]^{\cdot-}$ structure. This resulted in the formation of random finite magnetic chain segments imbedded onto the linear chains.[15] The dramatic, precipitous reduction of T_c with increasing $[CoCp^*_2]^+$ content is in excellent agreement with theoretical concepts,[16] Figure 2. With a 14.5% replacement of Co^{III} for Fe^{III}, the T_c dropped from 4.8 to 0.75 K.

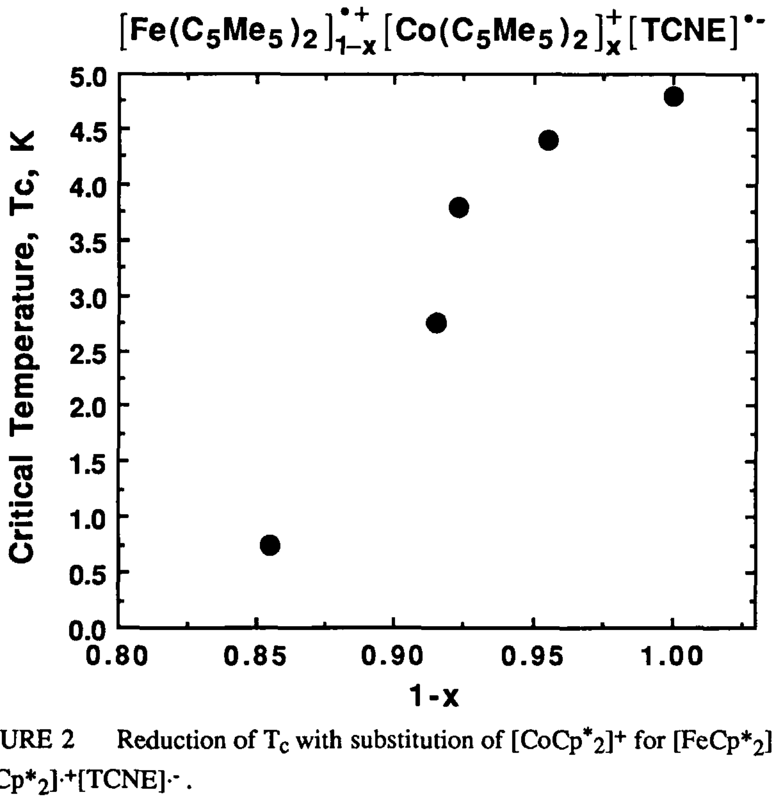

FIGURE 2 Reduction of T_c with substitution of $[CoCp^*_2]^+$ for $[FeCp^*_2]^{\cdot+}$ in $[FeCp^*_2]^{\cdot+}[TCNE]^{\cdot-}$.

Replacement of Fe^{III} in $[Fe^{III}Cp^*_2]^+[A]^{\cdot-}$ [A = TCNE, TCNQ] with doublet Ni^{III}, triplet Mn^{III}, or quartet Cr^{III} leads to compounds exhibiting antiferromagnetic, ferromagnetic, and ferromagnetic magnetic properties, respectively (*vide infra*).

With the goal of preparing additional molecular-based ferromagnets, the ferromagnetically coupled $[FeCp^*_2]^{\cdot +}[DDQCl_2]^{\cdot -}$ ($DDQCl_2$ = 2,3-dichloro-5,6-dicyanobenzoquinone) electron-transfer salt was characterized[17] (θ = +10 K). Since T_c is proportional to the spin magnitude (S), $[MnCp^*_2]^{:+}[DDQCl_2]^{\cdot -}$ was prepared anticipating that T_c might occur at temperatures accessible in our laboratories.[18] The high-temperature magnetic susceptibility of $[MnCp^*_2]^{\cdot +}[DDQCl_2]^{\cdot -}$ can be fit by the Curie-Weiss expression with a +26.8 K θ-value suggesting that the strongest exchange

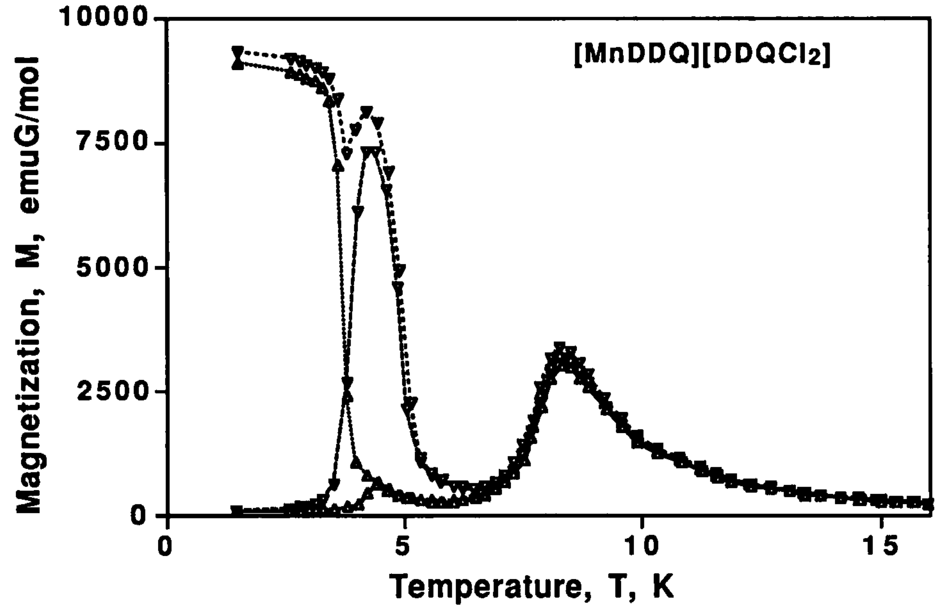

FIGURE 3 300 G molar magnetization, *M*, as a function of temperature for a zero-field (Δ, ∇) and high field (▲, ▼) cooled (previous aligned in 19.5 kG) polycrystalline sample of $[MnCp^*_2]^{:+}[DDQCl_2]^{\cdot -}$ as a function of increasing (Δ, ▲) and decreasing (∇, ▼) the magnetic field.

interactions (the interactions within individual chains) are ferromagnetic. Hysteretic magnetic field dependent behavior, albeit complex, was observed below ~7 K. The 150 to 2000 G magnetic field dependencies of the magnetization for a sample previously aligned in zero field or in high field (19.5 kG) is presented for increasing and decreasing magnetic fields, Figure 3. Above ~3.8 K the magnetization exceeds the expectation calculated from the Brilluoin function for fully aligned S = 1 and S = 1/2 spins with a dramatically different behavior at low temperatures. Thus, a complex magnetic phase diagram describes the system at low temperature, Figure 3. Assuming complete alignment of the crystals with magnetic field parallel to the C_5 molecular axis, a sample-history dependent saturation magnetization, M_s, is observed with values up to 24,200

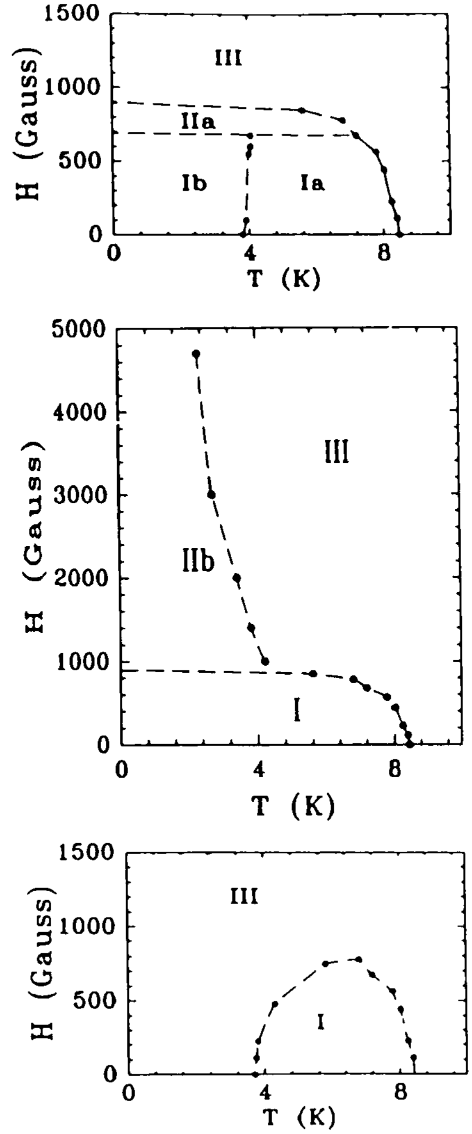

FIGURE 4 Magnetic phase diagram (see text) for $[MnCp^*_2]^{\cdot+}$-$[DDQCl_2]^{\cdot-}$ (from ref. 19).

emuG/mol. The data are consistent with strong ferromagnetic coupling between adjacent radicals within each chain and a net weak antiferromagnetic coupling between the chains.[19] This leads to metamagnetic behavior. Thus, when an applied magnetic field is large enough, it becomes energetically favorable for the spins in all the chains to align ferromagnetically. Below ~4 K there is an anomalous behavior with large hysteresis and remnant magnetization.[19] For example, at ~4 K the magnetization abruptly drops by more than an order of magnitude depending on the applied field to a value lower than calculated from the Brilluoin function. At high temperature there is a field dependent crossover from low magnetization to a high magnetization state. This is suggestive of the presence of perhaps both a metamagnetic and a possible lattice distortion (spin-Peierls-like) transitions. However, since spin-Peierls transitions occur only in antiferromagnetic states, complex magnetic behaviors must be operative for the material. Simple metamagnetic behavior has been reported for $[\mathrm{FeCp^*}_2]^{\cdot+}[\mathrm{TCNQ}]^{\cdot-}$ [9] and $[\mathrm{MnCp^*}_2]^{:+}$-$[\{\mathrm{M}[\mathrm{S_2C_2(CF_3)}]_2\}^{\cdot-}$ (M = Ni, Pd, Pt).[20]

From the experimental results three phase diagrams were derived to explain the various transitions. The equilibrium phase diagram for decreasing and increasing temperatures with the value of applied magnetic field being changed above an ordering temperature and kept constant during the temperature scan is presented in Figure 4a. There are three distinct regions: antiferromagnetic phase-I, mixed phase-II and the coexisting ferromagnetic-paramagnetic phase-III. A nonequilibrium phase diagram derived by cooling the sample in zero applied field above 8 K followed by increasing the applied magnetic fields at constant temperatures, Figure 4b. This diagram shows the first order boundary separating the different phases: the antiferromagnetic phase-I, the intermediate phase-IIb, and the ferromagnetic-paramagnetic phase-III. A nonequilibrium phase diagram for the metastable ferromagnetic state which appears after the system is cooled from 10 K in an applied field exceeding 1500 G to the desired temperature after which the field is decreased to the selected value and the temperature is subsequently reduced can be generated. This phase diagram is also achieved if a zero-field cooled sample is exposed to a sufficiently large external field, Figure 4c. The field is then decreased to the desired value and temperature is subsequently raised. The ferromagnetic state is stabilized at low fields (<650 G) below 4 K using this procedure.[19]

MODELS FOR MOLECULE-BASED MAGNETIC MATERIALS

Several mechanisms for obtaining the spin alignment throughout the solid necessary for ferromagnetism in a molecule/organic based material have evolved since the early 1970's. It is important to emphasize that the distinct mechanisms that have been proposed are for the pairwise stabilization of ferromagnetic coupling among spins and this is insufficient to account for three-dimensional ferromagnetic behavior, for which interactions in all three directions are crucial. The proposed models[21] include:

- Ferromagnetic exchange resulting from orthogonal orbitals (no CI) - Hund's rule
- Configuration Interaction (CI) to determined dominant ferro- or antiferromagnetic exchange
- Dipole-dipole (through-space) exchange not involving the overlap of orbitals

The CI model is complex with (a) excitations within a molecular species (intramolecular spin coupling) and (b) excitations between molecular species (intermolecular spin coupling). The latter can have excitations only involving the POMO on adjacent molecular species with or without spatial constraints. The CI model increases in complexity when the excitations involve NHOMO and/or NLUMO. Even greater mechanistic and computation complexity is involved when excitations between localized and delocalized (metallic) states (intramolecular spin coupling) are involved.

Frequently the exchange mechanisms are based on chemical stabilization of a spin state capable of exchange, leading to labeling of exchange mechanisms named by their chemical or physical nomenclature. An example of this approach is ferromagnetic exchange between polarons created in conjugated segments of block copolymers. In this case, polarons are the means in creating spin containing units. The exchange between these polarons comes from CI through the intervening moieties. The above is a classification of operative spin exchange mechanisms, not the means to achieve spins.

It is often unclear as to which mechanism is the primary exchange mechanism in a particular chemical system. Particularly for compositionally and structurally complex molecular species-based systems it is probable that more than one mechanism plays a significant role (e. g., ferromagnetic coupling of spins within a one-dimensional chain due to orthogonal orbitals (top mechanism) and ferromagnetic or antiferromagnetic coupling between chains due to configuration interaction (middle mechanism) or possibly dipole-dipole interactions between chains (bottom mechanism). Furthermore, since there are many levels of complexity of the CI model (bottom mechanism) there are many ways to describe this mechanism and exhaustive calculations are necessary to provide a detailed understanding.

It is important to emphasize that *highly magnetic behavior is not a property of a molecule, atom, or ion; it is a cooperative solid state (bulk) property.* Thus, to achieve bulk ferromagnetic behavior in the context of the aforementioned high-spin molecules, intramolecular interactions, perhaps as described above, must be operative or the molecule is sufficiently large to be itself a magnetic domain.

CALCULATION OF THE CURIE TEMPERATURE, T_C

Heisenberg along with Dirac[22a] solved expressions that relate T_C to exchange integral between site i and j, J, for the general spin case assuming that only the number of equivalent nearest neighbor sites, z, is important. This simplest mean-field model leads to the following expression for the general spin case.[22b]

$$T_c = \frac{2JzS(S+1)}{3k_B} \qquad [1]$$

where k_B is the Boltzmann constant.

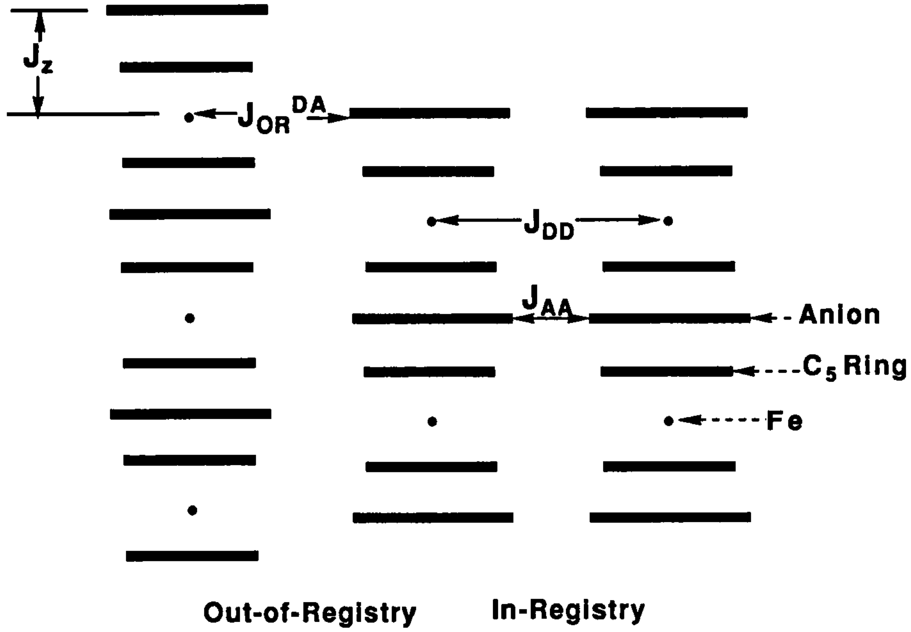

FIGURE 5 Schematic illustration of the structure of orthorhombic $[FeCp*_2]^{\cdot+}$-$[TCNE]^{\cdot-}$ showing intrachain pairwise out-of-registry and in-registry interactions.

This model is constrained to have only one spin site S and an unique J. These are poor assumptions for the $[MCp*_2]^+[TCNE]^{\cdot-}$ system as the distinct spin sites may have different values of *S* and the crystal structure implies four distinctly different nearest neighbor J's, i. e., J_Z, J_{AA}, J_{DD}, and $J_{or}{}^{DA}$, Figure 5. A more appropriate mean-field expression for T_c, *i. e.*, T_c =

$$\frac{64J_{eff}\left(S_AS_D + S_A^2S_D + S_AS_D^2 + S_A^2S_D^2\right)}{3\left[\sqrt{S_A^2 + 2S_A^3 + S_A^4 + S_D^2 + 2S_D^3 + S_D^4 + 34\left(S_AS_D + S_A^2S_D + S_AS_D^2 + S_A^2S_D^2\right)} - \left(S_A + S_A^2 + S_D + S_D^2\right)\right]}$$

as therefore developed.[23] Thus, assuming the inter- and interchain interactions remain unchanged as the donor is varied, the J_{eff} will remain constant and consequently the relative T_c can be calculated for different values of S_A and S_D, Table III. Clearly for $[Fe^{III}Cp*_2]^{\cdot+}[TCNE]^{\cdot-}$ T_c is $4J_{eff}$ within this mean-field model. Thus, since T_c is observed to be 4.8 K, then J_{eff} is 1.2 K. This result points out that the value of J_{eff} is indeed small, but sufficient to enable a T_c at experimentally accessible temperatures.

TABLE III

Calculated Mean-Field T_c as a function of S_D for $S_A = 1/2$ Systems

S_D	T_c	Scaled T_c[a]
1/2	4 J	1.00
1	6.8 J	1.70
3/2	10 J	2.50
2	13.7 J	3.43

[a] $T_c/T_c(S_D = 1/2)$

The key advantage of the above equation is that T_c can be scaled for different S_Ds, Table III. Thus, T_c for a $S_D = 1$ donor (with a $S_A = 1/2$ acceptor) is 6.8 J or 1.7 times greater than that for a $S_D = 1/2$ donor (with a $S_A = 1/2$ acceptor) system. Hence, since T_c is 4.8 K for $[\mathrm{Fe^{III}Cp^*_2}]^{\cdot+}[\mathrm{TCNE}]^{\cdot-}$, then all else being equal T_c would be expected to be 8.2 K for the isostructural $[\mathrm{Mn^{III}Cp^*_2}]^{:+}[\mathrm{TCNE}]^{\cdot-}$. This is in good agreement with the reported value of 8.8 K for $[\mathrm{Mn^{III}Cp^*_2}]^{:+}[\mathrm{TCNE}]^{\cdot-}$.[24] {More complex equations utilizing four different Js leads to an improved scaling of T_c as a function of S_D.}[23,24] Thus, the observed T_c is in excellent agreement with the experimental values and suggests that if this mean-field model is correct, then similar exchange interactions operate for both $[\mathrm{FeCp^*_2}]^{:+}[\mathrm{TCNE}]^{\cdot-}$ and $[\mathrm{MnCp^*_2}]^{:+}[\mathrm{TCNE}]^{\cdot-}$.

We also treated theoretically the $S_D = 3/2$ / $S_A = 1/2$ case {*i. e.*, $[\mathrm{CrCp^*_2}]^{:\cdot+}[\mathrm{TCNE}]^{\cdot-}$} and obtain a predicted scaled value for T_c of 12 K.[23] Experimental study of the magnetic susceptibility of the $[\mathrm{CrCp^*_2}]^{:\cdot+}[\mathrm{TCNE}]^{\cdot-}$ shows a ferromagnetic transition at 3.65 K[25] which is substantially lower than that of either $[\mathrm{FeCp^*_2}]^{\cdot+}[\mathrm{TCNE}]^{\cdot-}$ and $[\mathrm{MnCp^*_2}]^{:+}[\mathrm{TCNE}]^{\cdot-}$,. This trend is also observed for $[\mathrm{MnCp^*_2}]^{:+}[\mathrm{TCNQ}]^{\cdot-}$ ($T_c = 6.5$ K)[26] and $[\mathrm{CrCp^*_2}]^{:\cdot+}[\mathrm{TCNQ}]^{\cdot-}$ ($T_c = 3.5$ K).[20] The anomalously low value of T_c is further compounded by the ferromagnetic magnetic exchange, in contrast to the prediction of antiferromagnetic exchange and a ferrimagnetic ground state for the configuration mixing model described above (this model successfully yields the sign of the magnetic exchange of all other linear chain metallocene cases studied so far). Experimental study of the $[\mathrm{CrCp^*_2}]^{:\cdot+}[\mathrm{TCNE}]^{\cdot-}$ is complicated by its extreme sensitivity to the presence of oxygen which in turn modifies the observed exchange interactions.[25]

ROOM-TEMPERATURE POLYMERIC MAGNET

With the observation of bulk ferromagnetic behavior for $[\mathrm{MnCp^*_2}]^{:+}[\mathrm{TCNE}]^{\cdot-}$ the preparation of the electron-transfer salt of $\mathrm{V(C_6H_6)_2}$ and TCNE was identified for study.[27-29] $[\mathrm{V^I(C_6H_6)_2}]^{:+}$, like $[\mathrm{Mn^{III}Cp^*_2}]^{:+}$, is an $S = 1$ cation possessing a ${}^3E_{2g}$ ground state ($a_{1g}{}^1e_{2g}{}^3$).[30] Reaction of $\mathrm{V(C_6H_6)_2\cdot}$ with an excess of TCNE in dichloromethane results in an amorphous black precipitate with a nominal composition of V(TCNE)$_x$·yCH$_2$Cl$_2$ (x ~ 2; y ~1/2). However, due to the extreme insolubility of the precipitate and reactivity of the solvent and extreme air and water sensitivities, variations in composition as a function of preparation conditions have been observed. The first step in the reaction is electron transfer from V(C$_6$H$_6$)$_2$' to TCNE followed by loss of the benzene ligands. The material exhibits strong, broad absorptions at 2099 and 2188 cm^{-1} which are assigned to $\upsilon_{C\equiv N}$. The breadth of the $\upsilon_{C\equiv N}$ absorptions and their relatively low frequency are consistent with the presence of reduced TCNE, with nitrogens coordinated to vanadium.

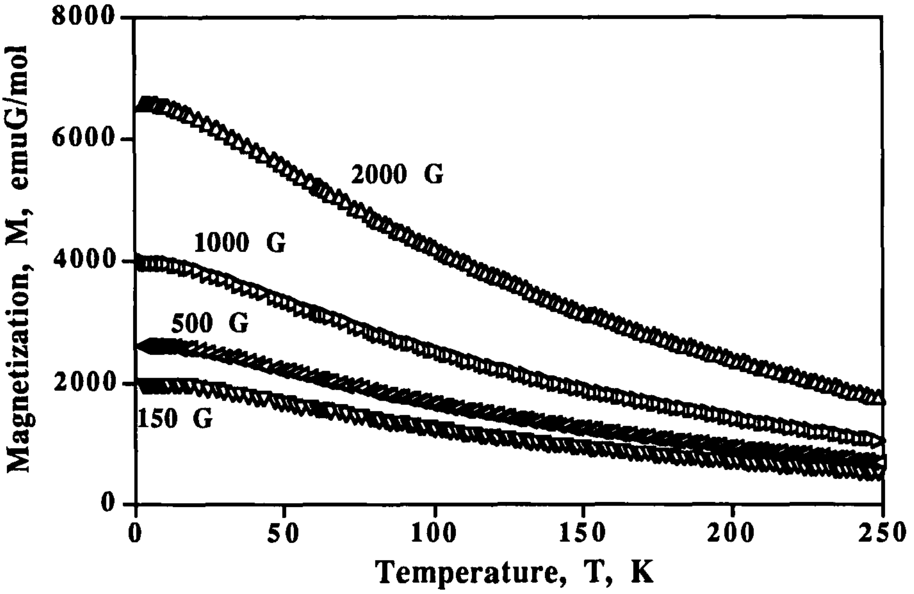

FIGURE 6 Magnetization, *M*, as a function of temperature, T, at different applied magnetic fields for V(TCNE)$_x$·y(CH$_2$Cl$_2$).

The V(TCNE)$_x$.y(CH$_2$Cl$_2$) has a field dependent magnetization, M, between 1.4 and 350 K, Figure 6. The unusual, nearly linear increase of *M* with decreasing temperature is unusual and may reflect the contribution of the two spin sublattices (V and TCNE) and/or the effects of disorder. Hysteresis with a coercive field of 60 G is observed at room temperature. The strong magnetic behavior is readily observed by its being attracted to a permanent magnet at room temperature, Figure 7. Thus, this system is the first and only example of molecular/organic based material with a critical temperature above room temperature. The critical temperature exceeds 350 K, the thermal decomposition temperature of the sample. A linear extrapolation of the magnetization to a temperature at which it would vanish leads to an estimate of a T$_c$ of

~400 K.[28,29] An independent estimate of T_c was obtained[29] using the empirical correlation between the spin wave coefficient and T_c exists for amorphous magnets.[31]

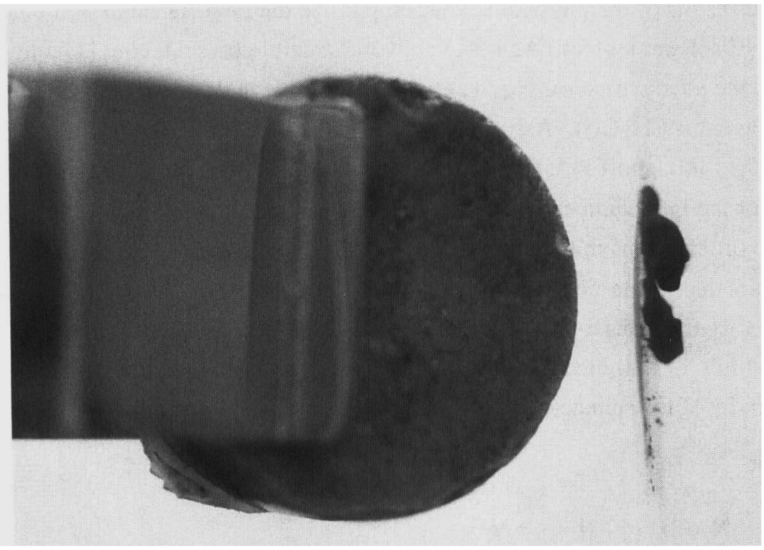

FIGURE 7 Photograph of a powdered sample of the magnet being attracted to a Co_5Sm magnet.

Due to the structural disorder and variable composition of the magnetic material, the structure has yet to be elucidated. TCNE may bond to metals in many ways. For early transition metals a linear or bent V-N σ-bonds are anticipated. Presently we formulate each vanadium as being surrounded by up to six ligands which are primarily N's from different TCNE's. Cl from the weak CH_2Cl_2 ligand or from oxidative addition of CH_2Cl_2 may also coordinate, Figure 8. Any trace oxygen that is present will strongly bond to the vanadium. The TCNE's may bind up to four different V's via σ-N bonds. This fragment may be planar or twisted (Figure 8); nonetheless, its ability to bind to more than one vanadium enables the construction of a 3-D network structure that supports strong 3-D spin-spin coupling necessary for a 400 K T_c. By using THF or MeCN as alternative solvents, materials with $T_c < 350$ K can be isolated and characterized. Given the geometrical constraints imposed by the coordination of TCNE to a metal ion, an open structure with unfilled vanadium coordination sites is not unexpected.

Although the structure is unknown, it is interesting to speculate as to the type of magnetic coupling present from this system. Based on the IR data and elemental analysis the precipitate appears to be best formulated as $V^{II}(TCNE)_2 \cdot 1/2(CH_2Cl_2)$ with $S = 3/2$ V^{II} and two $S = 1/2$ $[TCNE]^{\cdot -}$s. For ferromagnetic coupling S_{total} is 5/2 and assuming g is 2 the saturation magnetization, M_s, is expected to be 28 x 10^3 emuG/mol. For antiferromagnetic coupling between the V^{II} and the two $[TCNE]^{\cdot -}$'s and hence ferrimagnetic behavior the S_{total} is 1/2 and M_s is expected to be 5.6 x 10^3 emuG/mol.

This is in good agreement with the value of 6.0 x 10^3 emuG/mol observed at 2 K at 19.5 kG.[27-29]

The results of the physical studies emphasize the importance of 3-D coupling in the V/TCNE/solvent system. As a 3-D network structure present, eqn. [1] may be used to estimate the effective exchange interaction, J, operative in the room temperature magnet system (solvent = CH_2Cl_2). Assuming T_c = 400 K, S being the root-mean square of S_A (1/2) and S_D (3/2), and z = 5, then J_{eff} = 70 K. This is only 2.6 times greater than the J obtained for the intrachain exchange in $[\mathrm{FeCp}^*{}_2][\mathrm{TCNE}]$ for which T_c = 4.8 K, yet T_c is nearly two orders of magnitude greater. The differences in transition temperatures have in large part then to do not with the difference in J alone but also with the change in dimensionality from quasi-1-D to essentially a 3-D system. Hence, we conclude that for achieving high T_c in molecular/polymeric it is a significant advantage to increase the dimensionality of the spin network.

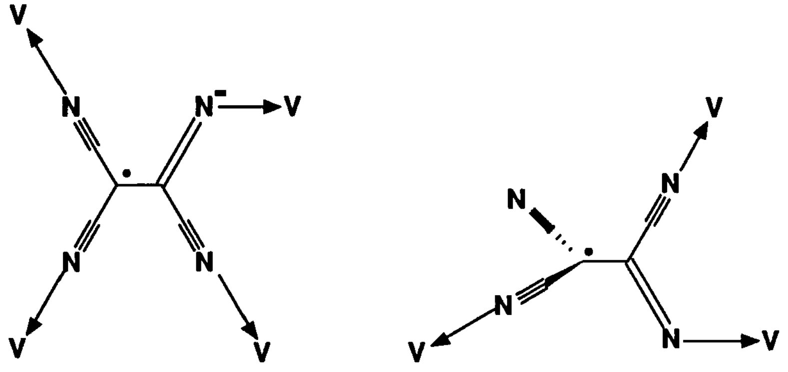

Planar Twisted

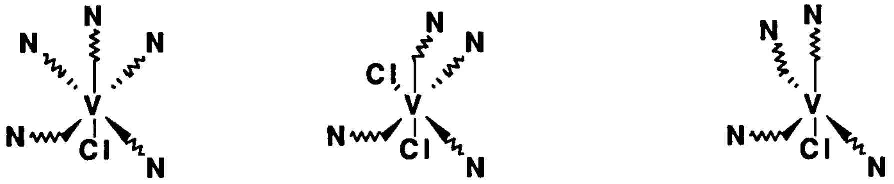

FIGURE 8 Proposed local bonding about each TCNE and V.

METALLOPORPHIN-BASED MAGNETS

$[\mathrm{MnTPP}]^{:+}[\mathrm{TCNE}]^{\cdot-}\cdot 2\mathrm{PhMe}$ (TPP = *meso*-tetraphenylporphinato) represents a new structural class of molecular magnets.[32] $[\mathrm{MnTPP}]^{:+}[\mathrm{TCNE}]^{\cdot-}\cdot 2\mathrm{PhMe}$ crystallizes as parallel 1-D $\cdots[\mathrm{D}]^{:+}[\mathrm{A}]^{\cdot-}[\mathrm{D}]^{:+}[\mathrm{A}]^{\cdot-}\cdots$ chains in which the $[\mathrm{TCNE}]^{\cdot-}$ binds identically to two $[\mathrm{MnTPP}]^{:+}$ moieties in a *trans*-μ_2-*N*-σ-bound fashion, Figure 9. The solid state motif is distinctly different than that for the $[\mathrm{MCp}^*{}_2]^+[\mathrm{A}]^{\cdot-}$ electron-transfer salts as $[\mathrm{TCNE}]^{\cdot-}$ does not coordinate to the M. Thus, the bonding of reduced TCNE to Mn is a model for the bonding of reduced TCNE to V in the $\mathrm{V[TCNE]_x{\cdot}y(solvent)}$ magnet.

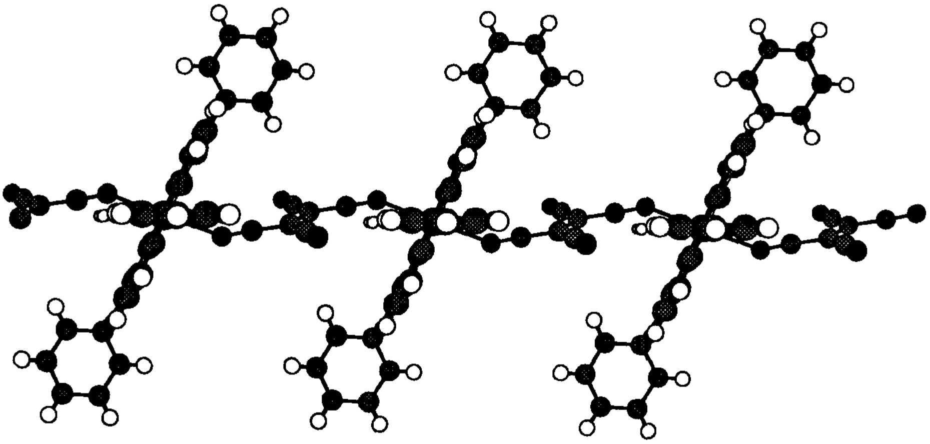

FIGURE 9 Segment of an 1-D $\cdots D^{+}A^{\cdot -}D^{+}A^{\cdot -}\cdots$ chain showing $[\mathrm{TCNE}]^{\cdot -}$ *trans*-μ_2-*N*-σ-bonding to $[\mathrm{MnTPP}]^{+}$ (the toluenes of solvation are not shown for clarity).

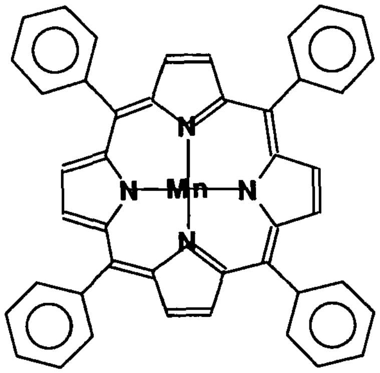

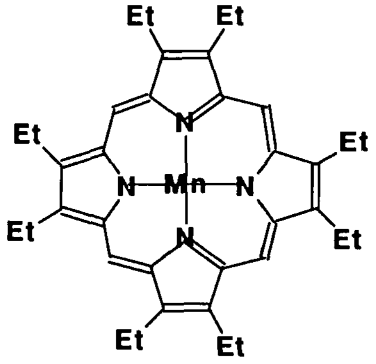

Manganesetetraphenylporphine, MnTPP

Manganeseoctaethylporphine, MnOEP

The susceptibility for $[\mathrm{MnTPP}]^{+}[\mathrm{TCNE}]^{\cdot -}\cdot 2\mathrm{PhMe}$ can be fit by the Curie-Weiss expression between 115 and 250 K ($\theta = +61$ K) and above 280 K ($\theta \sim -15$ K). Above 250 K the susceptibility exceeds expectation for independent spins. A minimum in the value of χT, characteristic of 1-D ferrimagnetic behavior,[33] is observed at ~310 K and field dependent susceptibility is observed below 50 K. The saturation magnetization, M_s, is up to 30,000 emuG/mol in good agreement for the expected saturation magnetization is 29,925 emuG/mol assuming ferromagnetic ordering of the $S = 1/2$ $[\mathrm{TCNE}]^{\cdot -}$ spin and $S = 2$ $[\mathrm{MnTPP}]^{+}$ spins. A hysteresis curve with a coercive field of 375 G was obtained at 5 K, demonstrating that [MnTPP][TCNE] is a magnet at low temperature. Extrapolation of the steepest slope of the 3 G M(T) data to zero yields an estimate of a magnetic ordering temperature of 18 K. Thus, [MnTPP][TCNE] with the *trans*-μ_2-*N*-σ-bonded $[\mathrm{TCNE}]^{\cdot -}$ is a representative example of a new structure type of molecular based magnetic materials. Due to the direct bonding of the TCNE to the Mns this class may also be an important model for the disordered room-temperature V/TCNE magnet.

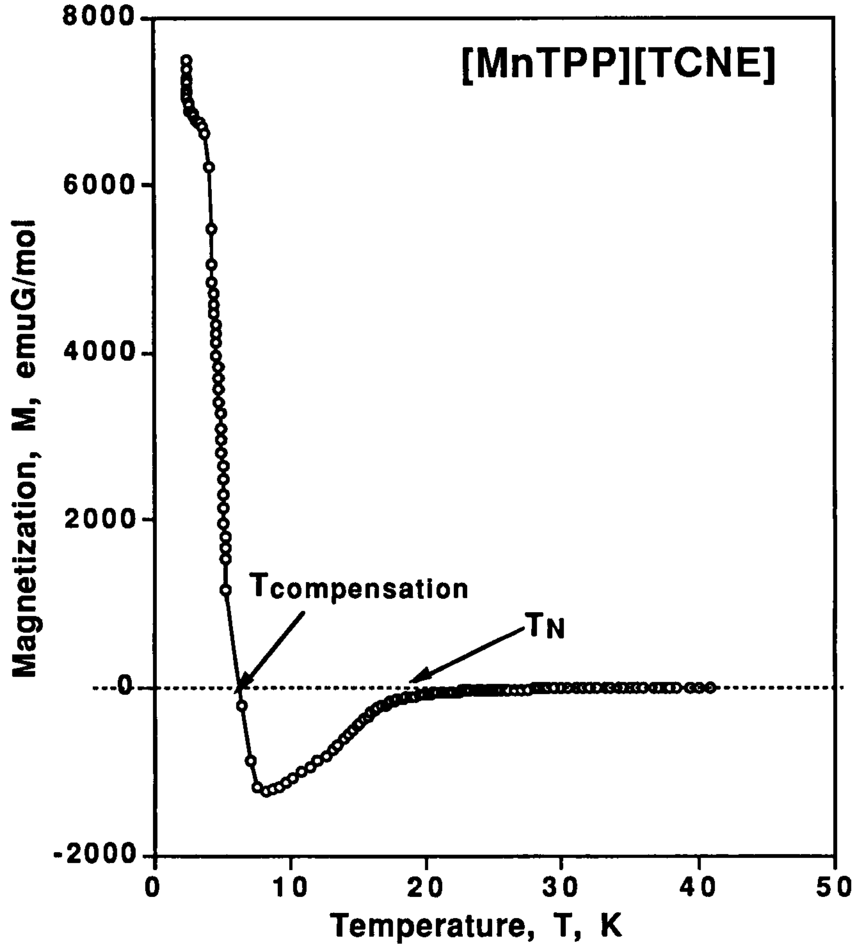

FIGURE 10 Remnant magnetization vs. temperature for $[MnTPP]^{\cdot+}[TCNE]^{\cdot-}\cdot 2PhMe$. The sample was cooled in an applied field of 11.5 kG to 2.1 K, then the applied field was reduced to zero, and magnetization was obtained while the sample was warmed (from ref. 34).

As a consequence of the alternating S = 2 and S = 1/2 chain structure, the $[MnTPP]^{\cdot+}[TCNE]^{\cdot-}\cdot 2PhMe$ 1-D chain is an excellent model system for studying a number of unusual magnetic phenomena, for example, the magnetic behavior of mixed quantum/classical spin systems.[34] Thus, $[MnTPP]^{\cdot+}[TCNE]^{\cdot-}\cdot 2PhMe$ shows a remarkable compensation phenomenon. That is, samples cooled in zero field, have a Neel ordering temperature at ~18 K. The sublattice magnetization within the two different spontaneous spin configurations vary differently under thermal activation, resulting in an unusual compensation phenomenon which mimics long range order, Figure 10.

To extend this system the analogous TCNE electron-transfer complex was prepared with the easier to oxidize MnOEP (OEP = octaethylporphine). $[\mathrm{MnOEP}]^{::+}[\mathrm{TCNE}]^{\cdot-}$ exhibits weak ferromagnetic coupling as evidenced by the fit of the susceptibility to the Curie-Weiss expression with a θ of +5 K. In contrast, however, this material does not exhibit any evidence for cooperative magnetic ordering down to 2 K. The differences in the magnetic properties lies in the structural differences. Although both $[\mathrm{MnTPP}]^{::+}[\mathrm{TCNE}]^{\cdot-}$ and $[\mathrm{MnOEP}]^{::+}[\mathrm{TCNE}]^{\cdot-}$ form parallel 1-D $\cdots[\mathrm{D}]^{::+}[\mathrm{A}]^{\cdot-}[\mathrm{D}]^{::+}[\mathrm{A}]^{\cdot-}\cdots$ chains, Figure 9, they are not uniform, but dimerized for $[\mathrm{MnOEP}]^{::+}[\mathrm{TCNE}]^{\cdot-}$. Also the π^* $[\mathrm{TCNE}]^{\cdot-}$ orbitals interact differently with the $\mathrm{Mn^{III}}$'s. Thus, uniform chains appear important for achieving long range magnetic order. This necessity has also been identified to achieve high, metal like dc electrical conductivity for 1-D molecule-based metals such as those based on TCNQ.

CONCLUSION

Since the initial reports of 3-D cooperative metamagnetism for $[\mathrm{FeCp^*_2}][\mathrm{TCNQ}]$ and ferromagnetism in $[\mathrm{FeCp^*_2}][\mathrm{TCNE}]$ there has been rapid, substantial progress in the synthesis of materials, models for the origin and control of the spin exchange interaction, and theories for the origin and details of the observed magnetic behavior such as T_C and saturation magnetization. The chronology of increases in T_C is compared to that of the organic and ceramic superconductors in Figure 11. From these exemplary materials exhibiting cooperative magnetic ordering the field of molecular/organic/polymeric based magnets has evolved to include a wide range of phenomena including magnetism in the V/TCNE molecular-based material significantly above of room temperature. As this research area has evolved, several chemical features have emerged as important considerations in designing new magnetic materials. Clearly to prepare a molecule-based magnet both the donor and acceptor, if present, must be radicals. Such radicals need only have one spin per site; however, a greater number of spins per site is expected to lead to higher T_C materials. For donor/acceptor based systems the competition between ferromagnetic and antiferromagnetic interactions arises from D···D, D···A, as well as A···A interactions. Subtle changes in the orbital overlaps presumably lead to subtle changes in magnetic coupling. Thus, akin to proteins, the primary, secondary, and tertiary structures are crucial for achieving the desired cooperative magnetic properties. Current limitations to the discovery of new molecular/organic/polymeric magnets requires the rational design of solid state structures which remains an art. This is due to the formation of numerous polymorphs, complex and solvated compositions, as well as undesired structure types. The growth of crystals enabling the study of the single crystal structure and magnetic properties is also an important limitation. With the dramatic rapid evolution of the field, major advances are expected to occur in this new arena of solid state science.

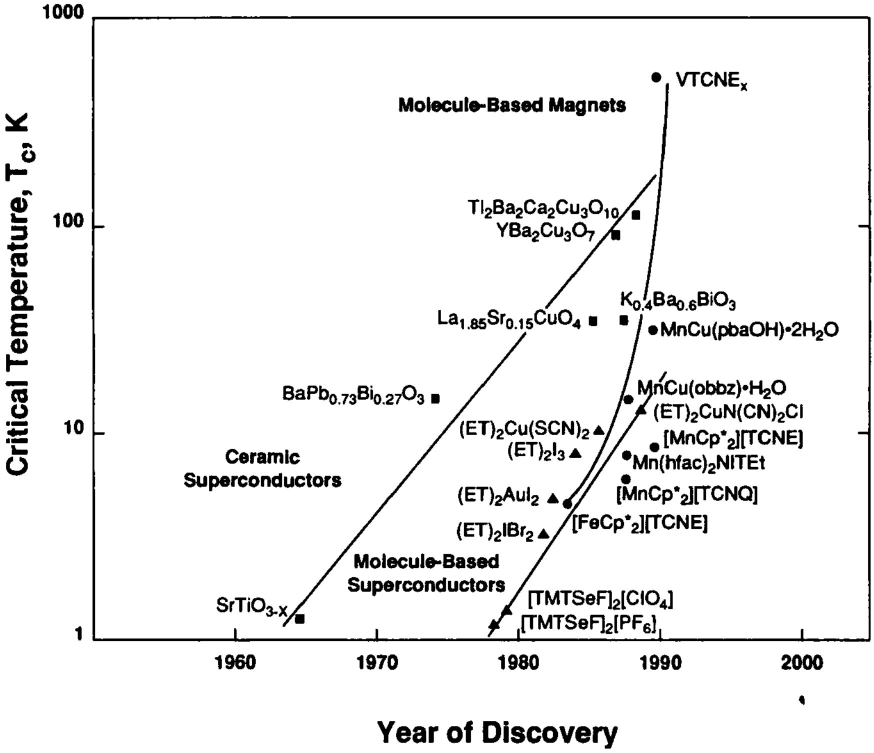

FIGURE 11 Time evolution of the discovery of increasing critical temperatures, T_C, for molecular-based magnetic materials as well as organic and oxide superconductors.

ACKNOWLEDGMENT

We have benefited greatly from the stimulating interactions and continued collaborations with our colleagues, postdoctoral fellows, and students for they have made important contributions enabling the rapid progress of the work reported herein. The authors furthermore gratefully acknowledge the support that the Department of Energy, Division of Materials Sciences (Grant No. DE-FG02-86BR45271) has given for these studies.

REFERENCES

1. A. Hellemans and B. Bunch, *Timetables of Science*, (Simon and Schuster, New York, NY, 1988), p19.
2. A. L. Buchachenko, *Russ. Chem. Rev.* *59*, 307 (1990); *Usp. Khim.* *59*, 529 (1990).

3. O. Kahn, *Structure and Bonding 68*, 89 (1987). O. Kahn and Y. Journaux, in press.
4. A. Caneschi, D. Gatteschi, R. Sessoli and P. Rey, *Acc. Chem. Res.* 1989, *22*, 392 (1989).
5. T. Sugawara, *Yuki Gos. Kag. 47*, 306 (1989).
6. J. S. Miller, A. J. Epstein and W. M. Reiff, *Acc. Chem. Res. 21*, 114 (1988). J. S. Miller, A. J. Epstein and W. M. Reiff, *Science 240*, 40 (1988). J. S. Miller and A. J. Epstein, *New Aspects of Organic Chemistry*, Z. Yoshida, T. Shiba and Y. Ohsiro, eds, VCH Publishers, New York, NY, 237 (1989). J. S. Miller, A. J. Epstein and W. M. Reiff, *Chem. Rev. 88*, 201 (1988).
7. J. S. Miller and A. J. Epstein, *Chemtech 21*, 168 (1991).
8. Proceedings on the Conference on *Ferromagnetic and High Spin Molecular Based Materials*, J. S. Miller and D. A. Dougherty, eds., *Mol. Cryst., Liq. Cryst. 176* (1989). Proceedings on the Conference on *Molecular Magnetic Materials*, O. Kahn, D. Gatteschi, J. S. Miller and F. Palacio, eds. *NATO ARW Molecular Magnetic Materials, E198* (1991).
9. G. A. Candela, L. Swartzendruber, J. S. Miller and M. J. Rice, *J. Am. Chem. Soc. 101*, 2755 (1979).
10. J. S. Miller, A. J. Epstein and W. M. Reiff, *Mol. Cryst., Liq. Cryst. 120,* 27 (1986).
11. E. Stryjewski and N. Giordano, *Adv. Phys.* 1977, *26*, 487.
12. J. S. Miller, J. C. Calabrese, H. Rommelmann, S. Chittapeddi, J. H. Zhang, W. M. Reiff and A. J. Epstein, *J. Am. Chem. Soc. 109*, 769 (1987).
13. S. Chittapeddi, K. R. Cromack, J. S. Miller and A. J. Epstein, *Phys. Rev. Lett. 58*, 2695 (1987).
14. Z. J. Huang, F. Chen, Y. T. Ren, Y. Y. Xue, C. W. Chu and J. S. Miller, submitted.
15. K. S. Narayan, K. M. Chi, A. J. Epstein and J. S. Miller, *J. Appl. Phys. 69,* 5953 (1991). K. S. Narayan, B. G. Morin, J. S. Miller and A. J. Epstein, *Phys. Rev. B 46,* 6195 (1992).
16. R. B. Stinchcombe, in *Phase Transitions and Critical Phenomena,* C. Domb and J. L. Lebowitz, eds. (Academic Press, London, UK), 7, 152 (1983).
17. E. Gerbert, A. H. Reis, Jr., J. S. Miller, H. Rommelmann and A. J. Epstein, *J. Am. Chem. Soc. 104*, 4403 (1982). J. S. Miller, P. J. Krusic, D. A. Dixon, W. M. Reiff, W. M. Zhang, E. C. Anderson and A. J. Epstein, *J. Am. Chem. Soc. 108,* 4459 (1986).
18. J. S. Miller, R. S. McLean, C. Vazquez, G. T. Yee, K. S. Narayan and A. J. Epstein, *J. Mat. Chem. 1*, 479 (1991).
19. K. S. Narayan, O. Heres, A. J. Epstein and J. S. Miller, *J. Magn. Magn. Mat. 110,* L6 (1992).
20. W. E. Broderick, J. A. Thompson and B. M. Hoffman, *Inorg. Chem. 30*, 2960 (1991).
21. J. S. Miller and A. J. Epstein, submitted.
22. (a) P. A. M. Dirac, *The Principles of Quantum Mechanics* (Oxford University Press, New York, 1935, 2nd Edition). P. A. M. Dirac, *Proc. Roy. Soc. 112A*, 661 (1926). (b) J. H. Van Vleck, *The Theory of Electric and Magnetic Susceptibilities*, Oxford University Press, London, 1932.
23. D. A. Dixon, A. Suna, J. S. Miller and A. J. Epstein, in *NATO ARW Molecular Magnetic Materials*, O. Kahn, D. Gatteschi, J. S. Miller and F. Palacio, eds. *E198*, 171 (1991).
24. G. T. Yee, J. M. Manriquez, D. A. Dixon, R. S. McLean, D. M. Groski, R. B. Flippen, K. S. Narayan, A. J. Epstein and J. S. Miller, *Adv. Mater. 3*, 309 (1991).
25. J. S. Miller, R. S. Mclean, C. Vazquez, J. C. Calabrese, F. Zuo, and A. J. Epstein, *J. Mat. Chem. 3*, 000 (1993). F. Zuo, S. Zane, P. Zhou, A. J. Epstein, R. S. McLean and J. S. Miller, *J. Appl. Phys. XX*, 000 (1993).
26. W. E. Broderick, J. A. Thompson, E. P. Day and B. M. Hoffman, *Science, 249,* 410 (1990).

27. J. M. Manriquez, G. T. Yee, A. J. Epstein, R. S. McLean, A .J. Epstein and J. S. Miller, *Science*, *252*, 1415 (1991).
28. (a) A. J. Epstein and J. S. Miller in the Proceedings of Nobel Symposium #NS-81 *Conjugated Polymers and Related Materials: The Interconnection of Chemical and Electronic Structure* (Oxford University Press, 1993) 475. (b) J. S. Miller, G. T. Yee, J. M. Manriquez and A. J. Epstein, in the Proceedings of Nobel Symposium #NS-81 *Conjugated Polymers and Related Materials: The Interconnection of Chemical and Electronic Structure*, Oxford University Press, 1993) 461.
29. A. J. Epstein and J. S. Miller, *Mol. Cryst., Liq. Cryst.* in press.
30. J. L. Robbins, N. Edelstein, B. Spencer and J. C. Smart, *J. Am. Chem. Soc.* 1982, *104*, 1882. F. G. N. Cloak, A. N. Dix, J. C. Green, R. N. Perutz and E. A. Seddon, *Organometallics 2*, 1150 (1983).
31. F. E. Luborsky, In *Ferromagnetic Materials*, E. P. Wohlfarth, ed. (North Holland Publishing Co., Amsterdam, 1980) *1*, 452.
32. J. S. Miller, J. C. Calabrese, R. S. McLean and A. J. Epstein, *Adv. Mat. 4*, 498 (1992).
33. *e. g.*, M. Verdauger, M. Julve, A. Michalowicz and O. Kahn, *Inorg. Chem. 22*, 2624 (1983). M. Drillon, J. C. Gianduzzo and R. Georges, *Phys. Lett. A 96A*, 413 (1983).
34. P. Zhou, A. J. Epstein, R. S. McLean, and J. S. Miller, *J. Appl. Phys. XX*, 000 (1993).